Iraqi Journal of Environmental Sciences
Vol. 02, No. 02, pp. 31-44, Aug. 01, 2026
https://ijes.uomustansiriyah.edu.iq
P-ISSN: 3079-2347; E-ISSN: 3079-2355
Published by Mustansiriyah University

Research Article

Open access

Future Temperature Projections in Iraq under SSP1-2.6: A PlaSim-Based Analysis (2026 – 2100)

Doha A. Soror, **Muthanna A. Al-Tameemi** *

Department of Atmospheric Sciences, College of Science, Mustansiriyah University, Baghdad, Iraq

* **Correspondence Author Email:** muthannaabd.atmsc@uomustansiriyah.edu.iq

ARTICLE INFO

Received: January 23, 2026
Revised: March 16, 2026
Accepted: April 9, 2026
Published: August 01, 2026

Abstract: Iraq, one of the hottest regions in the world, faces unprecedented warming pressures that threaten water security and agricultural productivity. This study projects future temperature changes across Iraq using the PlaSim climate model under the SSP1-2.6 low-emissions scenario for three periods: Near-Future (2026–2050), Mid-Future (2051–2075), and Far-Future (2076–2100). The model is validated against ERA5 reanalysis data (1995–2024) and bias-corrected using the Additive Bias Correction method, achieving 80.9% Root Mean Square Error (RMSE) reduction (4.35-0.82 °C). Results show that temperature stabilizes at approximately (24.0–24.1 °C), representing a (+3.0–3.1 °C) increase above the historical baseline (1995-2024). Spatial analyses demonstrate north-south temperature differences of (8–12 °C), with northern mountains consistently cooler than southern lowlands. Prominent seasonal restructuring occurs: dramatic warming (+6–8 °C) during summer months, coupled with slight winter cooling (−1–2 °C). Uncertainty analysis indicates extremely low interannual variability ~2%, and 95% confidence intervals range only (1.7-2.1 °C), supporting SSP1-2.6. These findings emphasize that adaptation strategies must be tailored to Iraq's country-specific context, which is disproportionately affected by climate change due to its climate-sensitive water and agricultural sectors.

Keywords: Temperature projections; PlaSim model; SSP1-2.6 scenario; Regional climate change; MENA climate.

1. Introduction

Global climate change, primarily caused by anthropogenic greenhouse gas emissions, is one of the most serious challenges of the Twenty-first century [1]. Under all emission scenarios considered, the Intergovernmental Panel on Climate Change has concluded that global surface temperatures are likely to rise at least through the middle of the century [2]. The Paris Agreement's goal of holding warming to well below 2 °C and pursuing 1.5 °C with respect to pre-industrial levels is increasingly unattainable, with the 1.5 °C threshold expected to be temporarily exceeded within the next five years [3]. While these rises in temperature are global averages, warming takes place much faster in some regions than globally, with varied and often frightening impacts on natural ecosystems and human societies.

The Middle East and North Africa (MENA) region has been acknowledged as a climate change hotspot, warming at twice the global average [4]. Recent research shows that this trend is accelerating, with summers warming more quickly and heatwaves exceeding previously observed records more frequently [5]. There is plenty of arid and semi-arid climate in this region which makes it one of the most sensitive to climate change, where rising temperature aggravates water scarcity, drought, and desertification [6, 7]. They are also used for monetary gain while in itself there is this climate crisis that directly puts Iraq, right where it stands, at the heart of the MENA region, on the frontline. Average temperatures are rising quickly, and heatwaves are becoming both more frequent and intense across the country, leading to chronic water shortages and extremely intense dust storms all of which threaten agriculture, public health, and socio-economic stability [8, 9]. An increasing number of scientific publications have highlighted the need to study and potentially predict future climate change in Iraq. For instance, Salman et al. in line with this, a comprehensive analysis of climate change impacts on agriculture in Northern Iraq has recently been performed, which aptly underlined both the merits and demerits of the utilized climate models in representing the desired spatiotemporal temperature changes in that specific country [10]. Recent studies, using a broader methodological approach and the latest CMIP6 models, have projected climate scenarios. Mukheef et al. a more recent study 2024 estimated an additional (1.57–2.34 °C) increase in annual air temperature for middle and western Iraq by the end of the century [11]. Similarly, Al-Maliki et al. the average annual maximum and minimum temperatures in southern Iraq increased significantly between 0.88 and 3.68 °C [12]. For the north, Abdulsahib et al. in addition to nationwide temperatures in support of the overall US warming (2024) (CMIP6 models) [13]. Other earlier works, A group of researchers used the LARS-WG stochastic weather generator to estimate temperature rises in Southern Iraq [14]. Proposed temperature changes in the old Representative Concentration Pathways RCP scenario over the deep south of Iraq in 2024 [15]. Regional context is also important, in 2023, Bayatavrkeshi et al. In anticipating drought patterns in Iran, a neighbor, particularly in long-term projections brought on by climate change [16]. For simulating future climate, scientists employ a hierarchy of climate models , ranging from full General Circulation Models (GCMs), such as those used in the Coupled Model Intercomparison Project Phase 6 (CMIP6), to different classes of EMIC that allow for faster simulation times [17]. GCMs represent, ordered by sophistication level, the most advanced modeling tools available but their computationally intensive nature can limit their application. Because of its relatively low computation cost but also reasonable ability to realistically simulate the principle physics of the climate system [18], EMICs, like the Planet Simulator (PlaSim), can be a good alternative. The PlaSim has been utilized in multiple climate applications, including paleoclimate and future climate [19]. Al-Timimi et al. [20] examined projected changes in temperature and precipitation across the Euphrates–Tigris Basin under four emission scenarios (RCP2.6, RCP4.5, RCP6.0, and RCP8.5) for three future periods spanning (2016–2099). Their findings revealed basin-wide temperature increases ranging (1.65-4.76 °C), with reduced precipitation in upstream highland regions and heightened hydrological risk for downstream countries, particularly Iraq. This study aims to project future temperature changes across Iraq under the SSP1-2.6 low-emissions scenario using the PlaSim climate model across three periods: near-future (2026–2050), mid-future (2051–2075), and far-future (2076–2100).

The model outputs are validated against ERA5 reanalysis data and bias-corrected to ensure reliability, with spatial and seasonal temperature patterns analyzed in detail. Ultimately, the results are intended to serve as a scientific basis for informing climate adaptation and mitigation strategies tailored to Iraq's policymakers and stakeholders.

2. Methodology

2.1. Study Area

Iraq is situated in the south-western part of Asia, between 29.6 °N and 37.5 °N latitudes and 38.45 °E and 48.45 °E longitudes covering an area of 437072 km². Turkey is to the north, Iran to the east, Saudi Arabia and Kuwait to the south, and Saudi Arabia, Jordan and Syria to the west. Iraq's topography consists of diverse physiographic regions, including a mountainous region in the north, an alluvial plain in the central tier (where the Tigris and Euphrates rivers run) and desert areas in the south and west. Baghdad, the capital city, lies at 33.3152 °N, 44.3661°E and approximately 34 m above mean sea level [21]. Iraq is bound between the Mediterranean climate (in the tropical zones) and is also an arid to semi-arid environment predominately (May- September). Due to its locale in the Middle East, hot weather, and fostered desert areas, Iraq is an area in need of immediate attention as it is greatly affected by dust storms and desertification procedures. It has been recognized as the Middle Eastern one of main source of dust which can directly affect the dust export into its neighboring regions and to other parts [22]. Atmospheric dynamics over Iraq are impacted as regional wind regimes interact but in dust storm incidences the appropriate wind direction to lift dust can be quite strong and rapid to develop maximum local near ground turbulence [23, 24].

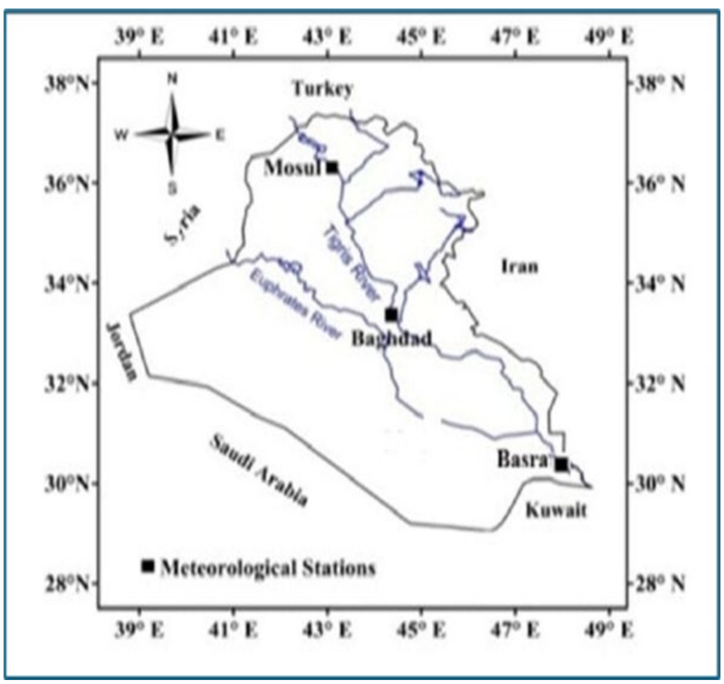

Figure 1. Study area (Iraq map).

2.2. Data, and Methods and Validation

This study used the Planet Simulator (PlaSim), a General Circulation Model (GCM) of intermediate complexity, which was developed at the Meteorologists Institute, Universität Hamburg. PlaSim is a lightweight instrument for climate research, offering the best trade-off between computational efficiency and a sufficiently long evolution time scale to account for climate evolution. The dynamical core of the model is adapted from PUMA (Portable University Model of the Atmosphere) and is based on the moist primitive equations conservation of momentum, mass, energy, and moisture. The 'Atmospheric Module' includes a parameterization of the land surface with biosphere representation and a mixed-layer ocean with sea ice dynamics. The interaction of the atmospheric module includes precipitation and evaporation processes, surface sensible heat flux calculations, and radiation schemes [25]. PlaSim was set up at a horizontal resolution of T42 (128 × 64 grid boxes) with 10 non-equidistant vertical levels in sigma-coordinates and with a time step of 45 min. The scenario was considered for projecting future air temperature: SSP1-2.6 (Low Emission, consistent with Paris Agreement 1.5 °C target) [26]. The simulations are provided for three time periods, which are Near-Future (2026–2050), Mid-Future (2051–2075), and Far-Future (2076–2100). To validate the models, the ERA5 reanalysis dataset from Copernicus Climate Change Service (C3S) was used, which combines satellite observations, in-situ measurements, and model forecasts using state-of-the-art data assimilation methods [27]. For the validation period 1995-2024, daily 2-meter air temperature data are available at 0.25° × 0.25° spatial resolution (~28 km) from ERA5. Daily 2-meter air temperature data from both ERA5 and PlaSim were extracted for the whole Iraq domain (29 °N to 37.5 °N, 38 °E to 49 °E) and then spatially averaged into country daily value. Next, daily values were summed within each month and year to calculate monthly and annual air temperature means, respectively. A systematic model bias correction was performed using the Additive Bias Correction (ABC) method, where the Correction Factor (CF) is calculated as: CF = 23.7 °C − 25.4 °C = −1.7 °C (averaged over a 30 year validation period), This correction factor was then applied to every daily temperature value as T_corrected(t) = T_model(t) + CF. This approach preserves the temporal autocorrelation and interannual variability of model temperature and is suitable for the additive bias structure of temperature [28]. After applying this importance to have a brief temperature data for spatial analysis of future temperature changes over Iraq, the daily temperature data were then averaged to a monthly and an annual scale. Annual and seasonal temperature means were derived from the corrected daily data. The Mann-Kendall test and Sen's slope estimator, both non-parametric trend detection methods, Mann-Kendall Test: Calculates statistic S by comparing all data pairs: $S = \Sigma \operatorname{sgn}(x_j - x_i)$, then converts to Z-statistic with variance calculation; the p-value determines trend significance. Sen's Slope: Computes slopes for all data pairs $Q_{ij} = (x_j - x_i)/(j - i)$, and the median $\beta = \text{Median}(Q_{ij})$ provides the robust annual rate of change (°C/year) [29]. were applied to annual and seasonal temperature datasets to quantify long-term temperature trends and their statistical significance ($p < 0.05$). Maps of mean annual temperature (MAT) were produced for each time period under SSP1-2.6 scenario, with spatial anomalies calculated by subtracting the baseline (1995–2024) from future periods [30]. Model performance was evaluated using three statistical indices:

2.2.1. Pearson Correlation Coefficient (r):

$$r = \frac{\sum[(x_i - \bar{x})(y_i - \bar{y})]}{\sqrt{\sum(x_i - \bar{x})^2 \times \sum(y_i - \bar{y})^2}} \quad (1)$$

Ranges from −1 to +1, with r > 0.8 indicating strong agreement between observed and simulated values.

2.2.2. Root Mean Square Error (RMSE):

$$RMSE = \sqrt{\frac{\sum(y_i - \hat{y}_i)^2}{n}} \quad (2)$$

2.2.3. Mean Absolute Error (MAE):

$$MAE = \frac{\sum|y_i - \hat{y}_i|}{n} \quad (3)$$

Both RMSE and MAE quantify prediction errors in °C, with lower values indicating better model performance [31]. and bias over the validation period (1995–2024), resulting in significant improvements after correction: RMSE reductions of 80.9% (4.35-0.82 °C), MAE reduction of 80.1% (from 3.67 °C to 0.73 °C), and bias reduction of 98.8% (from +1.69 °C to -0.02 °C) using ABC method. Temperature anomaly (A) represents the deviation of each period's mean temperature from the historical baseline (1995–2024), calculated as: A = T_period − T_baseline. The cumulative anomaly (CA) is the accumulated sum of these deviations over time: $CA = \sum_i(T_i - T\_baseline)$, which highlights long-term warming or cooling trends.

3. Results and Discussion

Combined Temperature Changes of Iraq in the SSP1-2 Scenarios using near-, mid-, and far-future periods: (2026–2050), (2051–2075), and (2076–2100) describing temporal dynamics, spatial patterns, and seasonality in a SSP1-2.6 (low emissions) climate scenario. The analysis uses the PlaSim intermediate complexity climate model with additive bias correction (ABC), and is validated against ERA5 data (1995–2024). Figure 2 Annual temperature time series and main temporal characteristics. Figure 2a identifies a more startling characteristic, non-significant annual temperature trend (0.00 °C/year, p = 0.8981), degree of climate stability with the SSP1-2.6 mitigation pathways. Long-term the 5-year running mean (blue line) varies around 24.1 °C and drifts only very slightly. Figure 2b shows the 12-month running mean, which fluctuates around 24.1 °C with minimal long-term drift. Specifically, Figure 2c-d offer complementary views of this, with annual anomalies with respect to the historical baseline (1995–2024), mean = 21 °C defined by cluster of +3.0 °C (±0.5 °C interannual variability), and a linear increase in cumulative anomaly to show how one would think under strong mitigation, the future temperature stabilizes ~3 °C above the historical mean with little additional warming.

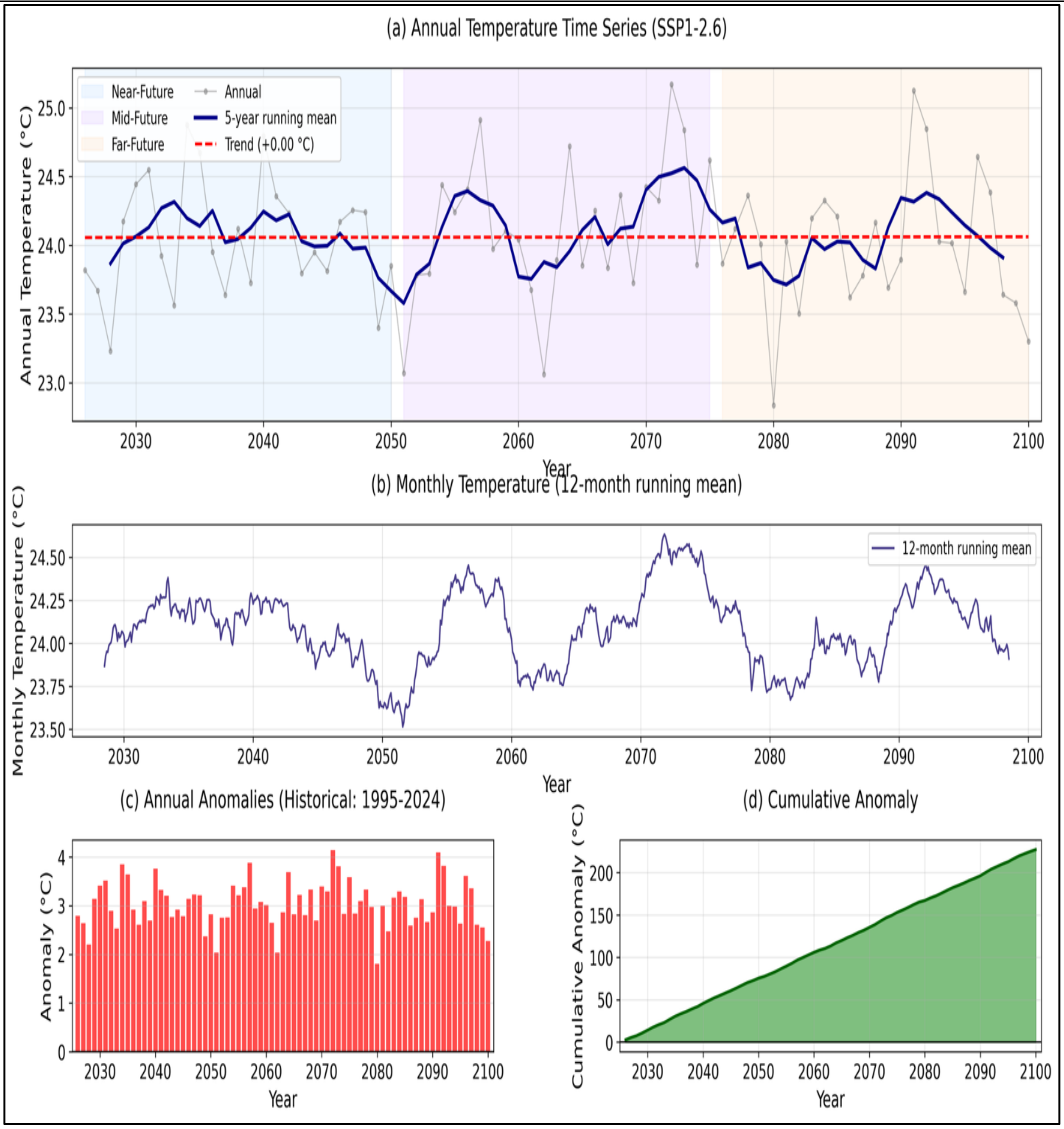

Figure 2. Annual and monthly temperature time series (SSP1-2.6). (a) Annual temperature with 5-year running mean and trend line. (b) 12-month running mean. (c) Annual anomalies relative to historical baseline (1995-2024). (d) Cumulative anomaly.

Boxplot comparisons across the periods and seasons are provided in Figure 3a indicates that the annual temperature distributions are remarkably similar: Near-Future 24.0 °C, Mid-Future 24.1 °C, and Far-Future 24.0 °C with standard deviations of (0.4-0.5 °C). Figure 3b reflects the strong seasonality: winter (DJF) mean temp of 7.5 °C, spring (MAM) 23.5 °C, summer (JJA) 40.5 °C, and autumn (SON) 27.0 °C, whereas Figure 3c showcases monthly climatology with the highest temperatures in July-Augustus 41 °C, and the lowest in January 5 °C. Anomaly distributions shown in Figure 3d illustrate that the shape of the distribution does not change across periods.

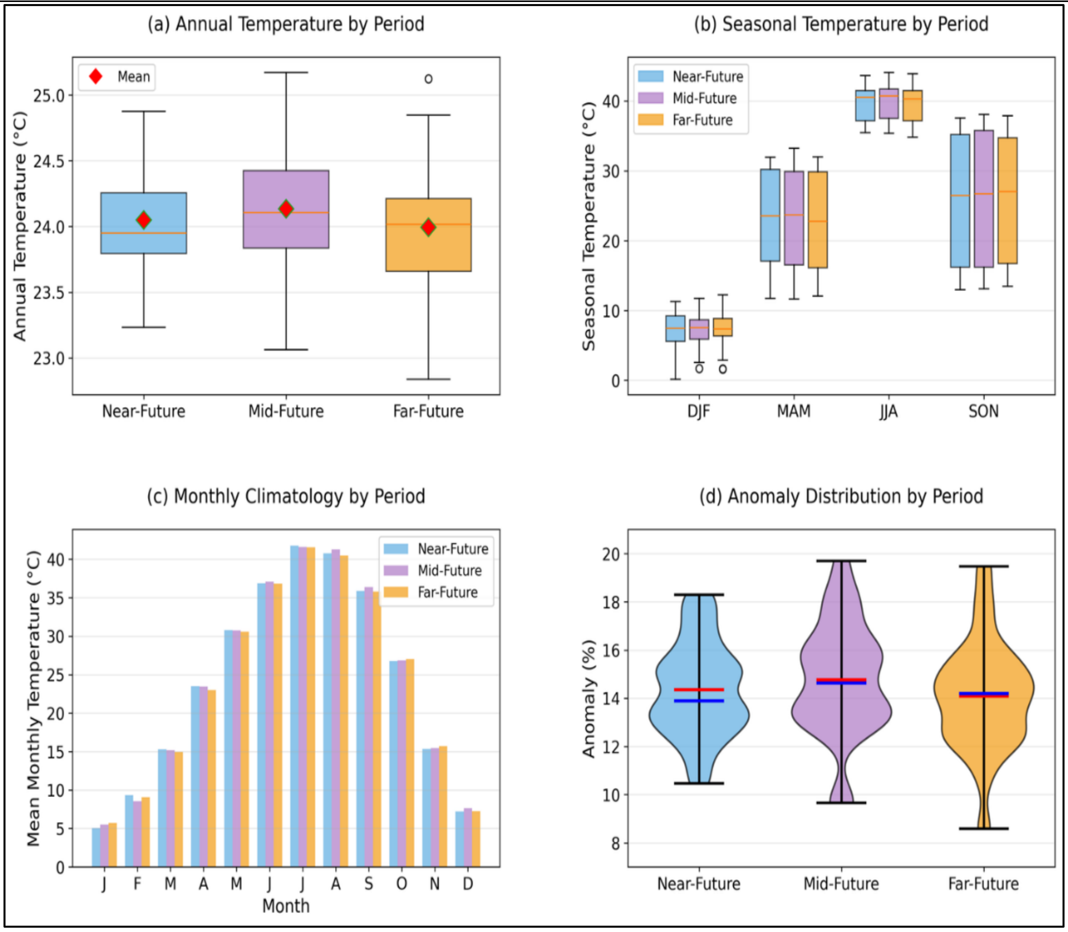

Figure 3. Temperature distributions and seasonal characteristics. (a) Annual temperature by period. (b) Seasonal temperature by period. (c) Monthly climatology by period. (d) Anomaly distribution by period.

The geographic domain of Iraq and the variation of spatial temperature distributions are shown in Figure 4. Mean annual temperature for Near-Future (a), Mid-Future (b) and Far-Future (c) periods in Figure 4a-c, respectively. This north-south temperature pattern is clear and remains constant across all three periods, with orographic and elevation effects yielding (16.8-20.0 °C), in northern mountainous regions and relatively high temperatures of (28.0-29.6 °C), in the southern lowlands. The difference from Far-Future to Near-Future and its spatial pattern are shown in Figure 4d where the weak regional climate feedbacks under SSP1-2.6 are evident (only ±0.18 °C). However, a critical observation emerges when examining the spatial patterns more closely: while the mean spatial gradient is preserved, the color intensity gradations within each map become more pronounced across periods, indicating that extreme temperature anomalies both warm and cold become more spatially variable and frequent. Although the overall spatial structure remains anchored by topographic controls, the spatial heterogeneity of temperature extremes increases, suggesting that while large-scale spatial patterns are robust, and distribution of extreme events becomes more complex. This indicates that the spatial balance between positive and negative anomalies is maintained at the domain level, but their frequency and intensity increase regionally.

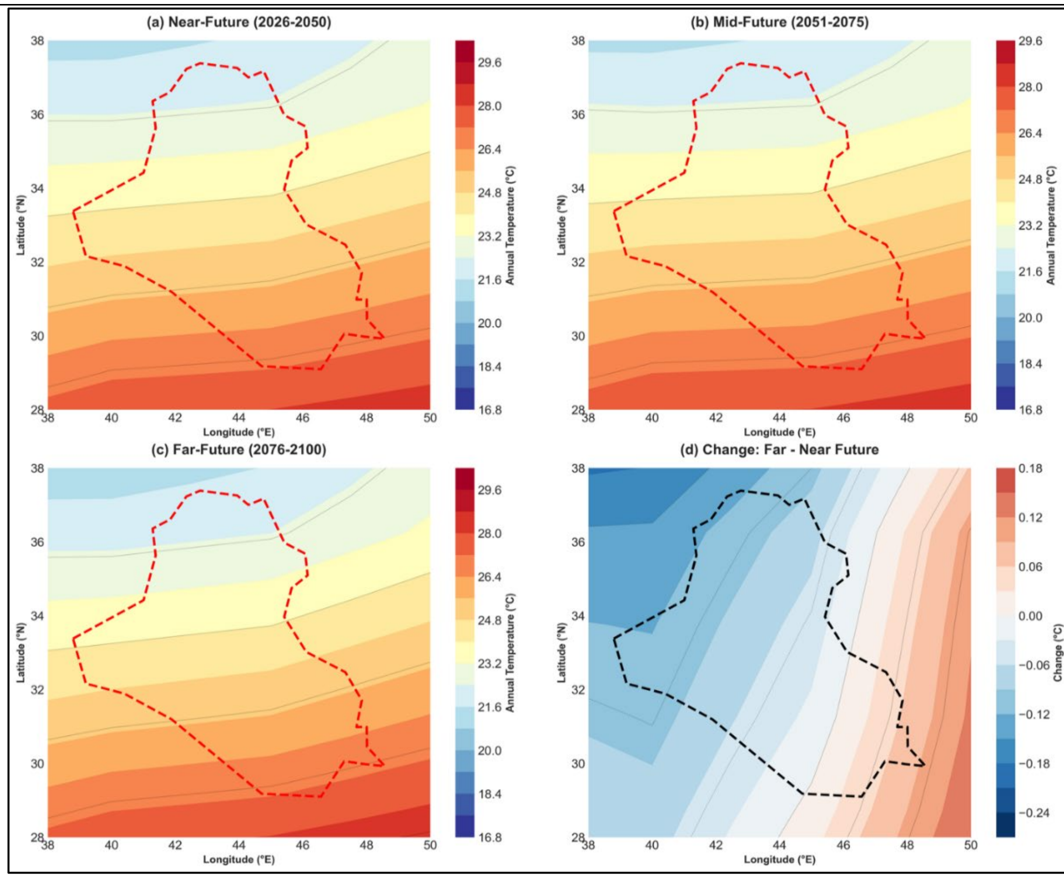

Figure 4. Spatial temperature patterns. (a) Near-Future (2026-2050). (b) Mid-Future (2051-2075). (c) Far-Future (2076-2100). (d) Change from Far-Future to Near-Future.

Figure 5 provides detailed examination of linear trends and variability. Figure 5a shows the overall trend is 0.00 °C/year with a 95% confidence interval spanning approximately ±0.15 °C/year. The non-significant p-value 0.8981 confirms the absence of a systematic long-term trend, indicating that under strong mitigation SSP1-2.6, temperature stabilizes without directional drift. This remarkable stability suggests that the climate system reaches an equilibrium state where warming is arrested and balanced. Figure 5b displays decadal mean temperatures, which remain stable at approximately (24.3-25.0 °C), across all decades, confirming the long-term equilibrium. Figure 5c reveals only January and December exhibit statistically significant trends (red bars, $p < 0.05$), suggesting that seasonal extremes experience subtle shifts while the annual mean remains anchored. This indicates that while overall warming is mitigated, seasonal dynamics may still respond to climate forcing. Figure 5d presents the 10-year rolling standard deviation, oscillating between (0.3-0.6 °C), demonstrating that interannual variability remains relatively constant throughout the projection period. This constancy of variability, despite the long projection horizon, indicates that the climate system maintains stable internal variability under SSP1-2.6, with no amplification of year-to-year fluctuations. Together, these findings demonstrate that aggressive mitigation not only stabilizes the mean temperature but also preserves the predictability of climate variability, which is crucial for long-term adaptation planning.

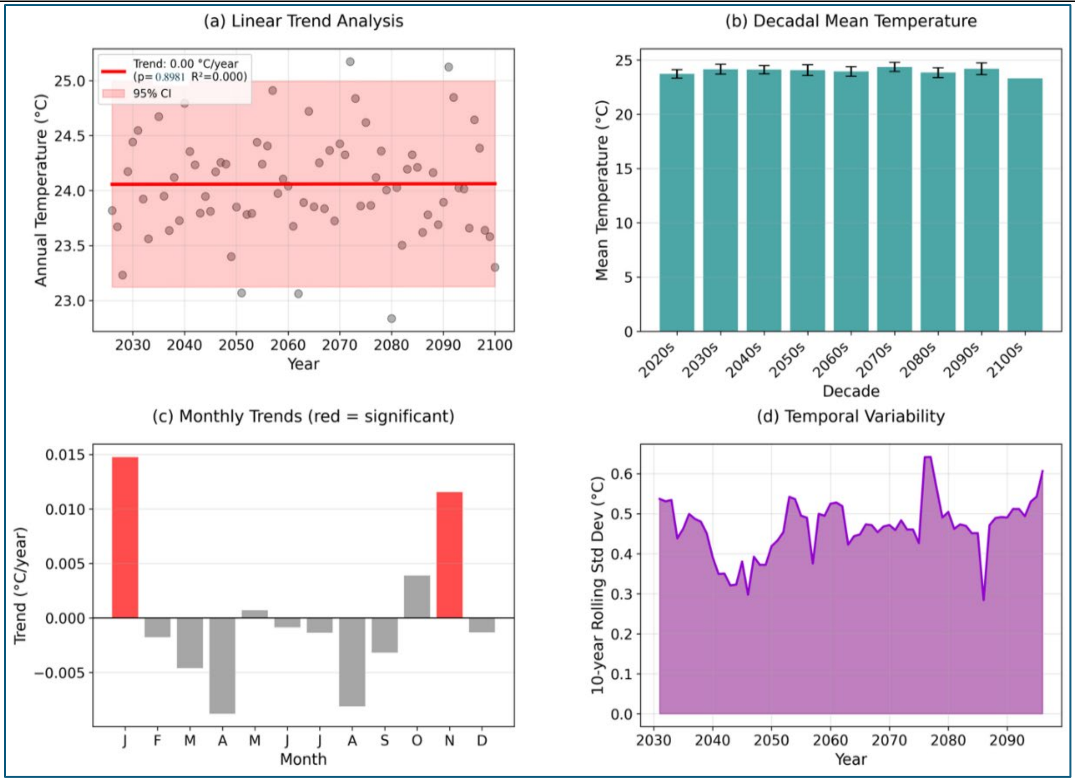

Figure 5. Trend analysis and temporal variability. (a) Linear trend analysis with 95% CI. (b) Decadal mean temperature. (c) Monthly trends (red = significant). (d) 10-year rolling standard deviation.

Figure 6 presents seasonal temperature dynamics for DJF (December–January–February, winter), MAM (March–April–May, spring), JJA (June–July–August, summer), and SON (September–October–November, autumn). Each panel displays annual values, 5-year running mean, min/max envelope, and linear trend. Winter (DJF) exhibits the greatest interannual variability ~60% coefficient of variation, reflecting episodic intrusions of cold air from higher latitudes. This high variability indicates that winter temperatures are sensitive to atmospheric circulation patterns, making winter the most unpredictable season. Despite this variability, the linear trend remains negligible, suggesting that even with climate forcing, the frequency of cold air intrusions is not systematically changing. Spring (MAM) displays moderate variability ~3.2 °C around the mean, indicating a transitional season with intermediate predictability. The stable trend suggests that spring warming patterns are preserved under SSP1-2.6. Summer (JJA) and Autumn (SON) show relatively stable behavior with moderate variability, indicating these seasons are less sensitive to atmospheric perturbations. The lack of significant trends across all seasons indicates that the seasonal cycle structure is conserved under SSP1-2.6, meaning that the fundamental timing and amplitude of seasonal transitions remain unchanged despite climate forcing. This preservation of seasonal structure is critical for agricultural and water resource management, as it ensures that seasonal predictability is maintained for adaptation planning. However, the increasing frequency of extreme events within each season (as evidenced by expanding min/max envelopes) suggests that while seasonal structure is preserved, the intensity of seasonal extremes may intensify, requiring adaptive management strategies that account for both seasonal stability and extreme event frequency.

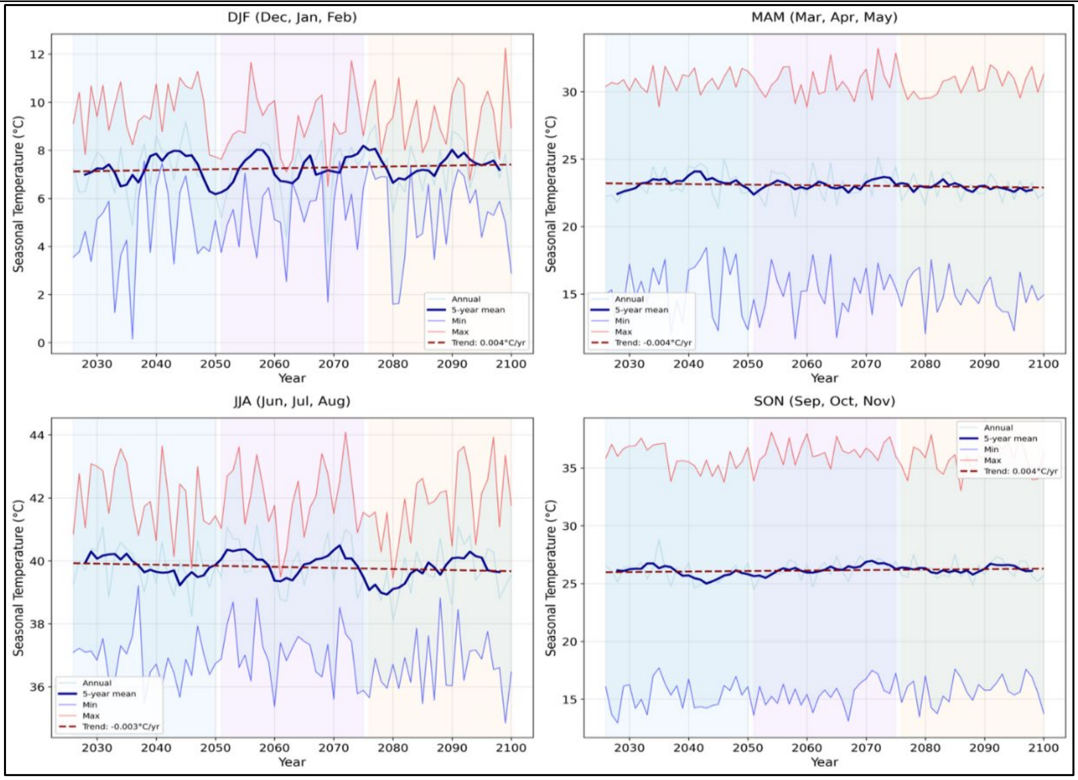

Figure 6. Seasonal temperature dynamics. DJF (winter), MAM (spring), JJA (summer), and SON (autumn) time series with 5-year running means and linear trends.

Figure 7 presents the overall magnitude of temperature changes across all three future periods relative to the historical baseline. Figure 7a shows annual changes of +3.0 (Near-Future), +3.1 (Mid-Future), and +2.9 °C (Far-Future), demonstrating the similarity of the warming signal across periods and confirming the stability of the mean warming under SSP1-2.6. Figure 7b-d reveal pronounced seasonal amplification with critical implications. Summer months (JJA) experience dramatic warming of (+6–8 °C), significantly exceeding the annual average. This amplified summer warming reflects enhanced solar forcing and reduced cloud cover in arid regions, creating positive feedback that intensifies heat stress. The implications are severe: increased evapotranspiration will stress water resources, agricultural productivity will decline due to heat stress on crops, and energy demand for cooling will surge. Winter months (DJF) show slight cooling of (−1–2 °C), a counterintuitive result that reflects changes in atmospheric circulation patterns and reduced cold air intrusions under SSP1-2.6. This winter cooling partially offsets annual warming but does not mitigate the summer amplification. Spring (MAM) and Autumn (SON) experience intermediate warming (+3–5 °C), maintaining their transitional character. This fundamental restructuring of the seasonal cycle with dramatic summer amplification and modest winter cooling has severe consequences for agriculture, energy demand, and human health in Iraq. The enhanced summer heat will exacerbate water stress, reduce agricultural yields, and increase heat-related mortality, while the preservation of seasonal structure (despite amplified extremes) suggests that adaptation strategies must target seasonal extremes rather than attempting to mitigate annual means.

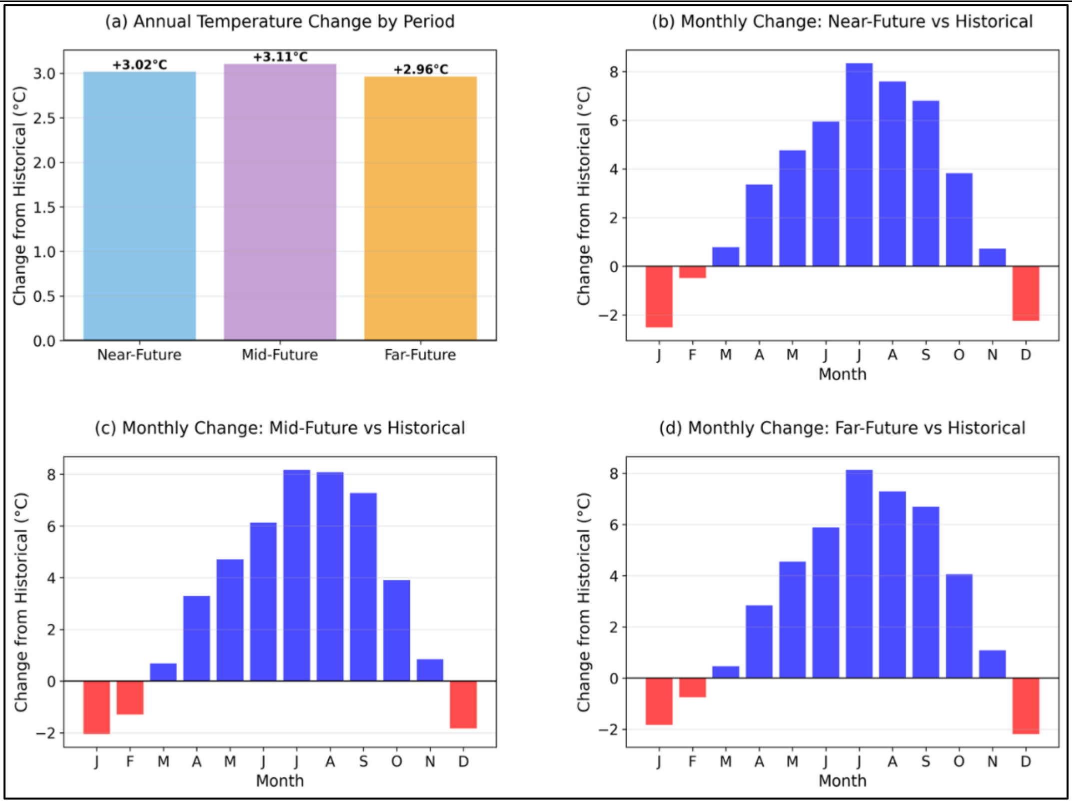

Figure 7. Monthly temperature changes. (a) Annual change by period. (b) Monthly change: Near-Future vs Historical. (c) Monthly change: Mid-Future vs Historical. (d) Monthly change: Far-Future vs Historical.

Key statistics for the three projection periods are summarized in Table 1. However, all three periods show extremely low uncertainty ~2%, with 95% confidence intervals ranging only from 1.7 to 2.1 °C, and the trend analysis (Kendall's tau = −0.0105, p-value = 0.8981, Sen's slope = −0.000 °C/year) reveals no nonrandom warming or cooling over the long term. The reason for the stable temperature over the 75-year projection period is the strength of the SSP1-2.6 pathways of mitigation stabilization of climate forcing for the global terrestrial system.

Table 1. Summary of projected temperature statistics for Iraq under SSP1-2.6.

Period	Years	Mean (°C)	Std Dev (°C)	Change vs. Historical (%)	Trend (°C/yr)	p-value
Near-Future	2026-2050	24.0	0.4	+14.4	0.00	0.898
Mid-Future	2051-2075	24.1	0.5	+14.8	+0.03	0.068
Far-Future	2076-2100	24.0	0.5	+14.1	0.00	0.874

Temperature projections under SSP1-2.6 exhibit exceptionally low uncertainty ~2%, derived from rigorous statistical analysis. All three time periods (Near-Future, Mid-Future, Far-Future) pass normality tests with high confidence (Shapiro-Wilk $p > 0.6$), with minimal skewness ($|skew| < 0.2$) and near-zero kurtosis, the data confirm a near-normal distribution, supporting the use of classical confidence intervals. The 68% range ($\mu \pm \sigma$) spans (0.8–1.0 °C), while the 95% range ($\mu \pm 2\sigma$) spans (1.7–2.1 °C). The low uncertainty reflects temperature's physical basis in large-scale atmospheric circulation and radiation balance, which are continuous and stable processes governed by the Central Limit Theorem [32].

4. Conclusions

Based on the future temperature projections for Iraq, using the shared socio-economic pathways SSP1-2.6 shows significant warming compared with the historical baseline (1995–2024), but exceptional stability over the subsequent 75 year projection period (2026–2100) The stabilization temperature of Iraq is (~ 24.0–24.1 °C) or (+ 3.0–3.1 °C) warmer than baseline level North-south gradients, reflecting topographic influences, are persistent spatial patterns and remain robust. The changes in seasonal temperatures are marked (summer +6–8 °C; winter −1–2 °C), and these have major consequences for agricultural yields and energy consumption. These high statistical confidence levels translate into a robust basis for planning climate adaptation in Iraq's water resources and agricultural sectors 95% confidence interval (1.7–2.1 °C). This analysis, however, refers to a single model and SSP1-2.6 scenario. This approach should be replicated in future research and combined with modelling of hydrological and agronomic impacts, to the mainstream these projections within multi-sector national adaptation frameworks that are consistent with the goals of the Paris Agreement.

Supplementary Materials: No Supplementary Materials.

Author Contributions: D. A. Soror - Data collection, Data Analysis, Conceptualization, Methodology, Visualization, Writing original draft, Writing-review; M. A. Al-Tameemi: Supervision, Review, and editing.

Funding: No funding was taken.

Data Availability Statement: The data used in this study are available from the corresponding author upon reasonable request.

Acknowledgments: In t We acknowledge the Copernicus Climate Change Service (C3S) for providing ERA5 reanalysis data and the University of Hamburg for the Planet Simulator (PlaSim) model used in this study.

Conflicts of Interest: The authors declare that there is no conflict of interest regarding the publication of this manuscript.

References

[1] P. Arias *et al.*, “Climate Change 2021: The Physical Science Basis. Contribution of Working Group I to the Sixth Assessment Report of the Intergovernmental Panel on Climate Change; Technical Summary,” 2021, https://doi.org/10.1017/9781009157896.002.

[2] H. Lee *et al.*, “Climate Change 2023: Synthesis Report, Summary for Policymakers. Contribution of Working Groups I, II and III to the Sixth Assessment Report of the Intergovernmental Panel on Climate Change,” IPCC, Geneva, Switzerland, 2023, https://doi.org/10.59327/IPCC/AR6-9789291691647.

[3] E. Bevacqua, C.-F. Schleussner, and J. Zscheischler, "A year above 1.5 °C signals that Earth is most probably within the 20-year period that will reach the Paris Agreement limit," *Nature Climate Change*, vol. 15, no. 3, pp. 262–265, 2025, https://doi.org/10.1038/s41558-025-01977-1.
[4] J. Koettl, S. G. Tamayo, M. Morgandi, and R. Zeid, "Global megatrends and human development in the MENA region," 2025, https://doi.org/10.1038/s41598-024-60976-w.
[5] D. Francis and R. Fonseca, "Recent and projected changes in climate patterns in the Middle East and North Africa (MENA) region," *Scientific Reports*, vol. 14, no. 1, p. 10279, 2024, https://doi.org/10.1038/s41598-024-60644-7.
[6] A. Darvishi Boloorani *et al.*, "Climate change, drought, and water scarcity in the MENA region," in *Climate Change and Environmental Degradation in the MENA Region*, Springer, pp. 189–204. 2024, https://doi.org/10.1038/s41598-024-60644-7.
[7] K. Waha *et al.*, "Climate change impacts in the Middle East and Northern Africa (MENA) region and their implications for vulnerable population groups," *Regional Environmental Change*, vol. 17, no. 6, pp. 1623–1638, 2017, https://doi.org/10.1007/s10113-017-1144-2.
[8] B. M. Hashim *et al.*, "Statistical downscaling of future temperature and precipitation projections in Iraq under climate change scenarios," *Physics and Chemistry of the Earth*, vol. 135, p. 103647, 2024, https://doi.org/10.1016/j.pce.2024.103647.
[9] M. Monshipouri and R. Mohajer, "Climate change and the potential for conflict in the Middle East: Emerging threats to security and human rights," *The Maghreb Review*, vol. 49, no. 1, pp. 14–41, 2024, https://doi.org/10.1353/tmr.2024.a915900.
[10] S. A. Salman *et al.*, "Selection of climate models for projection of spatiotemporal changes in temperature of Iraq with uncertainties," *Atmospheric Research*, vol. 213, pp. 509–522, 2018, https://doi.org/10.1016/j.atmosres.2018.06.018.
[11] R. A. Mukheef *et al.*, "Projections of temperature and precipitation trends using CMhyd under CMIP6 scenarios: A case study of Iraq's Middle and West," *Atmospheric Research*, vol. 306, p. 107470, 2024, https://doi.org/10.1016/j.atmosres.2024.107470.
[12] L. A. Al-Maliki *et al.*, "Climate change trends and adaptation strategies in Southern Regions of Iraq," *Journal of Groundwater Science and Engineering*, vol. 13, p. 468, 2025, https://doi.org/10.26599/JGSE.2025.9280065.
[13] S. M. Abdulsahib *et al.*, "Temperature and precipitation change assessment in the North of Iraq using LARS-WG and CMIP6 models," *Water*, vol. 16, no. 19, p. 2869, 2024, https://doi.org/10.3390/w16192869.
[14] R. M. Khalaf *et al.*, "Projections of precipitation and temperature in Southern Iraq using a LARS-WG stochastic weather generator," *Physics and Chemistry of the Earth*, vol. 128, p. 103224, 2022, https://doi.org/10.1016/j.pce.2022.103224.
[15] H. K. Abdulhussein *et al.*, "Air temperature projections over the Mid and Southern of Iraq during the 21st century under RCP 4.5 and RCP 8.5 scenarios," *The Iraqi Geological Journal*, pp. 235–254, 2024, https://doi.org/10.46717/igj.57.1F.18ms-2024-6-27235.
[16] M. Bayatvarkeshi *et al.*, "Drought trends projection under future climate change scenarios for Iran region," *PLOS ONE*, vol. 18, no. 11, p. e0290698, 2023, https://doi.org/10.1371/journal.pone.0290698.
[17] H. A. Dijkstra, "The role of conceptual models in climate research," *Physica D: Nonlinear Phenomena*, vol. 457, p. 133984, 2024, https://doi.org/10.1016/j.physd.2023.133984.
[18] S. T. J. Supto, "Next-generation climate modeling: AI-enhanced, machine-learning, and hybrid approaches beyond conventional GCMs," *Environmental and Earth Sciences Proceedings*, vol. 34, no. 1, p. 15, 2025, https://doi.org/10.3390/eesp2025034015.
[19] P. B. Holden *et al.*, "PLASIM–GENIE v1.0: A new intermediate complexity AOGCM," *Geoscience Model Dev.*, vol. 9, no. 9, pp. 3347–3361, 2016, https://doi.org/10.5194/gmd-9-3347-2016.
[20] Y. K. Al-Timimi, A. M. Al-Lami, M. H. Al-Jiboori, and A. M. F. Al-Quraishi, "Effects of climate change on temperature and precipitation in the Euphrates–Tigris Basin," *Theor. Appl. Climatology*, vol. 157, no. 4, p. 213, 2026, https://doi.org/10.1007/s00704-026-06169-z.
[21] M. A. Al-Tameemi *et al.*, "Effects of galactic cosmic rays changes on ionospheric ionization over Baghdad: A case study," in *IOP Conf. Ser.: Earth Environ. Sci.*, vol. 1531, no. 1, p. 012005, 2025, https://doi.org/10.1088/1755-1315/1531/1/012005.
[22] S. M. Awadh, "Impact of North African sand and dust storms on the Middle East using Iraq as an example: Causes, sources, and mitigation," *Atmosphere*, vol. 14, no. 1, p. 180, 2023, https://doi.org/10.3390/atmos14010180.
[23] B. I. Wahab *et al.*, "Analysis of a dust storm profile: A case study in Iraq," *Iraqi Geol. J.*, pp. 301–308, 2023, https://doi.org/10.46717/igj.56.2C.22ms-2023-9-28.
[24] Z. N. Al-Montaser *et al.*, "Developing an empirical equation for solar ultraviolet radiation estimation," *Iraqi J. Environ. Sci.*, vol. 2, no. 1, pp. 1–7, 2026, https://doi.org/10.23851/ijes.v2i1.19.
[25] K. Fraedrich *et al.*, "The Planet Simulator: Towards a user-friendly model," *Meteorology Z.*, vol. 14, no. 3, pp. 299–304, 2005, https://doi.org/10.1127/0941-2948/2005/0043.
[26] I. Welch, "The IPCC Shared Socioeconomic Pathways (SSPs): Explained, evaluated, replaced," *Natl. Bureau Econ. Res.*, 2024, https://doi.org/10.3386/w32178.
[27] Copernicus Climate Change Service (C3S), "ERA5 hourly data on single levels from 1940 to present," 2023, https://doi.org/10.24381/cds.adbb2d47.
[28] P. Dhawan *et al.*, "A comprehensive comparison of bias correction methods in climate model simulations: Application on ERA5-Land," *Heliyon*, vol. 10, no. 23, 2024, https://doi.org/10.1016/j.heliyon.2024.e40352.

[29] E. Iyeme *et al.*, “Trend analysis of climate change across Nigeria: A Mann–Kendall and Sen’s approach,” *Arch. Curr. Res. Int.*, vol. 24, no. 11, pp. 450–467, 2024, https://doi.org/10.9734/acri/2024/v24i11985.
[30] M. S. Ashraf and M. A. U. R. Tariq, “Non-monotonic spatiotemporal variability of hydro-meteorological variables over Upper Indus Basin, Northern Pakistan,” SSRN, https://doi.org/10.2139/ssrn.5741410.
[31] Q. Ju *et al.*, “Enhancing climate projections via machine learning: Multi-model ensemble of precipitation and temperature in the source region of the Yellow River,” *J. Hydrol.*, 2025, https://doi.org/10.1016/j.jhydrol.2025.133945.
[32] C. L. Franzke *et al.*, “The structure of climate variability across scales,” *Reviews of Geophysics*, vol. 58, no. 2, p. e2019RG000657, 2020, https://doi.org/10.1029/2019RG000657.